ELSEVIER

Carbohydrate Research 279 (1995) 41–57

CARBOHYDRATE RESEARCH

Investigation of the conformational properties of a β-(1 → 3) branched β-(1 → 6) heptasaccharide elicitor and its analogues by internal coordinate stochastic dynamics

Michael G. Petukhov *, Alexey K. Mazur, Lyudmila A. Elyakova

Pacific Institute of Bioorganic Chemistry, The Russian Academy of Sciences, 690022, Vladivostok, Russian Federation

Received 20 January 1994; accepted in revised form 5 July 1995

Abstract

A series of β-(1 → 3) branched β-(1 → 6) oligosaccharides that are known to take part in switching immune reactions in plants was studied by a molecular dynamics approach. A novel technique was applied which recently proved to be very efficient in polypeptide simulations. Molecular dynamics is simulated in internal rather than Cartesian coordinates with dramatically reduced numbers of degrees of freedom and a time step ten-fold larger than usual values. Comparison and classification of most populated conformational states revealed a few conformational motifs that are frequently adopted by highly active oligosaccharides and are not populated in an inactive analogue. As a result a putative biologically active conformation of the oligosaccharides is proposed.

Keywords: Conformational states; Branched oligosaccharides; Internal coordinate stochastic dynamics

1. Introduction

The term "elicitor" was introduced [1] to describe substances that, even at concentrations as low as 10^{-8} g per one gram of plant, stimulate biosynthesis of plant antibiotics (phytoalexins) in quantities sufficient to inhibit growth of microbial pathogens [2].

β-(1 → 3) Branched β-(1 → 6) gluco-oligomers of different lengths represent a well-characterized class of elicitors. Another term, oligosaccharins, has been introduced

* Corresponding author. Present address: Department of Organic Materials, Osaka National Research Institute, AIST, Ikeda, Osaka 563, Japan.

SSDI 0008-6215(95)00277-4

by Albersheim et al. [3] to describe oligosaccharides that can regulate the triggering of plant defence against pathogens. There are several types of these substances. Branched β-oligosaccharides are among the most potent elicitor oligosaccharins discovered so far. These substances were first detected in the 1970s [4], but studies of their primary structures took nearly 10 years.

The oligosaccharides considered here were isolated from an oligosaccharide mixture resulting from the partial acid hydrolysis of mycelial cell walls of *Phytophthora megasperma f. sp. glycinea*. It was found [5] that the smallest oligosaccharin that had full activity was a heptasaccharide elicitor (HSE) having the following primary structure:

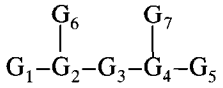

1

where G_i denotes β-D-glucosidic residues and "–" and "|" denote β-(1 → 6) and β-(1 → 3) bonds, respectively. Here and below, G_1 is always a non-reducing terminus of the main chain.

Compound **1** was the only elicitor-active compound in the mixture of approximately 300 heptasaccharides having very similar structures. In particular, it was shown that the following oligosaccharides were almost elicitor inactive [5].

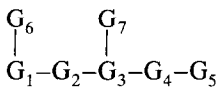

2a

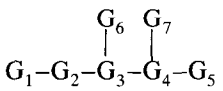

2b

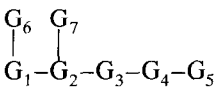

2c

Hahn et al. [6] investigated elicitor activity of several synthetic oligoglucosides structurally related to HSE. They showed that even minor chemical modifications of the non-reducing terminus of HSE destroys its elicitor activity even though bulk modifications at the reducing end have only small effects.

The structure of HSE has also been confirmed by synthesis [7]. The synthesized compounds had exactly the same NMR and CD characteristics and exhibited elicitor activity [8].

Unfortunately, there are as yet no experimental data concerning the spatial structure of these molecules in water or when bound with a receptor. It should be expected that the biological activity of these substances is connected with some specific conformational motifs that can be adopted by HSE. Such motifs may also be present in longer chains that include such fragments, but would be sterically prohibited or weakly populated in structures **2a**, **2b**, **2c**, and other inactive analogues.

In this work we have obtained molecular dynamics trajectories for HSE and for its two analogues having the following structures:

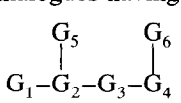

3a

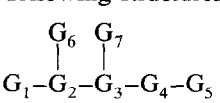

3b

These substances have been tested earlier for elicitor activity [6]. Compound **3a** had approximately the same activity as HSE, while the heptaglucoside analogue (**3b**) was active only in concentrations approximately 1000-times higher than HSE. Based on comparison of the ensembles of possible conformations of these three molecules, we have attempted to identify probable structural factors important for elicitor activity.

2. Experimental

Empirical potential.—All atoms of the oligosaccharide models were treated explicitly. The geometry of the glucosidic residues was taken from the work of Takeda et al. [9]. The geometry parameters of β-(1 → 6) and β-(1 → 3) glycosidic linkages were: O-1–C-6′ bond length, 1.453 Å; C-1–O-1–C-6′ bond angle, 114°; O-1–C-6′–C-5′ bond angle, 108.7°; and C-1–O-1–C-3 bond angle, 118°. Here the ′ symbol refers to the next residue along the polysaccharide chain. Other bond angles and bond lengths were fixed at their crystal values. All parameters for the non-bonded interactions were taken from ECEPP parameter set [10–12]. Van-der-Waals, electrostatic, hydrogen bond, and torsion potentials were included in the energy calculations. Electrostatic energies were computed from Coulomb's law. Partial charges were taken from ab initio calculations [13]. Solvent screening effects were simulated by use of a dielectric constant $\varepsilon = 81$ (see discussion below). The torsion rotation contributions were calculated from the standard ECEPP expression:

$$U(\theta) = (U_0/2)(1 + \cos 3\theta)$$

Barrier heights were taken as 2.7 kcal/mol for CH–CH_2 bonds and 0.6 kcal/mol for CH–OH and CH–O bonds [10]. The exo-anomeric effect was neglected. To avoid the necessity to renew interaction lists during molecular dynamics and energy minimization the complete list of non-bonded interactions of the molecule under investigation was used. The glucosidic rings were fixed in the $^4C_1$ conformation. During molecular dynamics the ϕ, ψ, ω angles of the glucosidic linkages, torsions of CH_2OH groups, and hydroxyl torsion angles were varied. The ϕ, ψ, and ω torsions in the β-(1 → 6) glucosidic linkages are defined here by the following atoms: ϕ, H(C-1)–C-1–O-1–C-6′; ψ, C-1–O-1–C-6′-C-5′; ω, O-1–C-6′–C-5′–H(C-5′).

Although the ECEPP force field is specific for polypeptides it has been successfully used for conformational analysis of protein–carbohydrate complexes as well as individual oligosaccharides [14,15]. Moreover, in a recent detailed comparative study [16] it was shown that ECEPP predicts coupling constants for β-xylobiose in water more accurately than other more specific force fields (MM2 and MM2CARB). Somewhat earlier it was shown that only the van der Waals component of ECEPP could serve as a good first approximation for selection of putative solution conformations [17]. The underlying idea is that in any conformation of a small molecule in water all hydrogen bonding valences are occupied while electrostatic interactions, including the exo-anomeric effect, are reduced due to high solvent polarizability. Our approach is essentially similar because, by introducing a high dielectric constant to ECEPP, we dramatically reduce the contribution of both electrostatic and hydrogen bonding forces.

In order to validate the choice of ECEPP as the first approximation force field for our studies, we built up conventional energy maps for β-gentiobiose and laminarabiose and compared them with earlier published maps obtained with MM3 potentials. In Fig. 1, six ECEPP maps for gentiobiose are presented which are analogous to those reported by Dowd et al. [18] (see Fig. 5 of ref. [18]). One can see that: (i) the partial volumes of the conformational space corresponding to the main conformational substates are approximately the same with both potentials; (ii) the locations of energy minima are similar on ECEPP and MM3 maps; (iii) both in ECEPP and MM3 maps the crystal conformation of β-gentiobiose [19] is very close to the second lowest energy minimum. Energy maps are extended along the ψ direction (in the range of 60–300°), indicating high variability of this torsion angle. At the same time it is apparent that the energy ranking of the minima corresponding to the main rotamers about the O-1–C-6′ bond is $gt < gg < tg$ in MM3 and $tg < gg < gt$ in ECEPP. In both cases, however, all minima are within an energy interval of 2 kcal/mol. Also, there are several high energy regions on ECEPP maps that do not exist on MM3 maps, which indicates generally higher flexibility of the oligosaccharide with the MM3 potential. The higher rigidity of ECEPP is a clear consequence of fixed bond lengths, bond angles, and sugar cycle conformation. We note, however, in the course of molecular dynamics simulations all rotamers about the O-1–C-6′ bonds were observed and it was clear that relative populations of *gt–gg–tg* states are determined by tertiary interresidue contacts rather than by local interactions.

A similar comparison was made for laminarabiose studied earlier by Dowd et al. [20]. The computed ECEPP map (Fig. 2) has one broad global minimum which is close to both the crystal structure [21] and the global minimum in the MM3 potential [20]. The second best minimum at (158°, 16°) corresponds to the third one observed in MM3 [20]. On MM3 maps there is one more minimum at (36°, 169°), 3 kcal/mol above the global one. In the case of ECEPP, there is also a local minimum at this point but its energy is much higher (17 kcal/mol) due to close interresidue contacts, H(C-1)–H(C-2′) and H(C-1)–H(C-4′). The latter observation is a very clear effect of a fixed C-1–O-1–C-3 bond angle in ECEPP. The last minimum could not be sampled in our calculations, but it is not likely to have a significant effect on the conformational properties of the molecules being studied.

To conclude the description of the potential, we note that in any vacuum simulation of chain molecules compact conformations always predominate due to attractive van der Waals interactions. In water the oligosaccharides studied may be even more compact or unfolded due to hydration forces that are not well understood and so far cannot be simulated reliably. Although the analysis of possible hydration effects is beyond the scope of our studies, we note that the oligosaccharides considered are large enough to exhibit weak amphiphilic properties. In many conformations discussed below, the stacking of sugar residues provides a significant van der Waals contribution to the total energy, but in water the same stacking may be favoured by the hydrophobic effect. We believe, therefore, that one can sensibly assume that the ensemble of compact conformations observed in vacuum simulations is not dramatically different from that in solution.

Internal coordinate stochastic dynamics.—Recently, a new approach for effective scanning of the conformational space of chain molecules has been developed: Internal Coordinate Stochastic Dynamics (ICSD). Unlike traditional molecular dynamics meth-

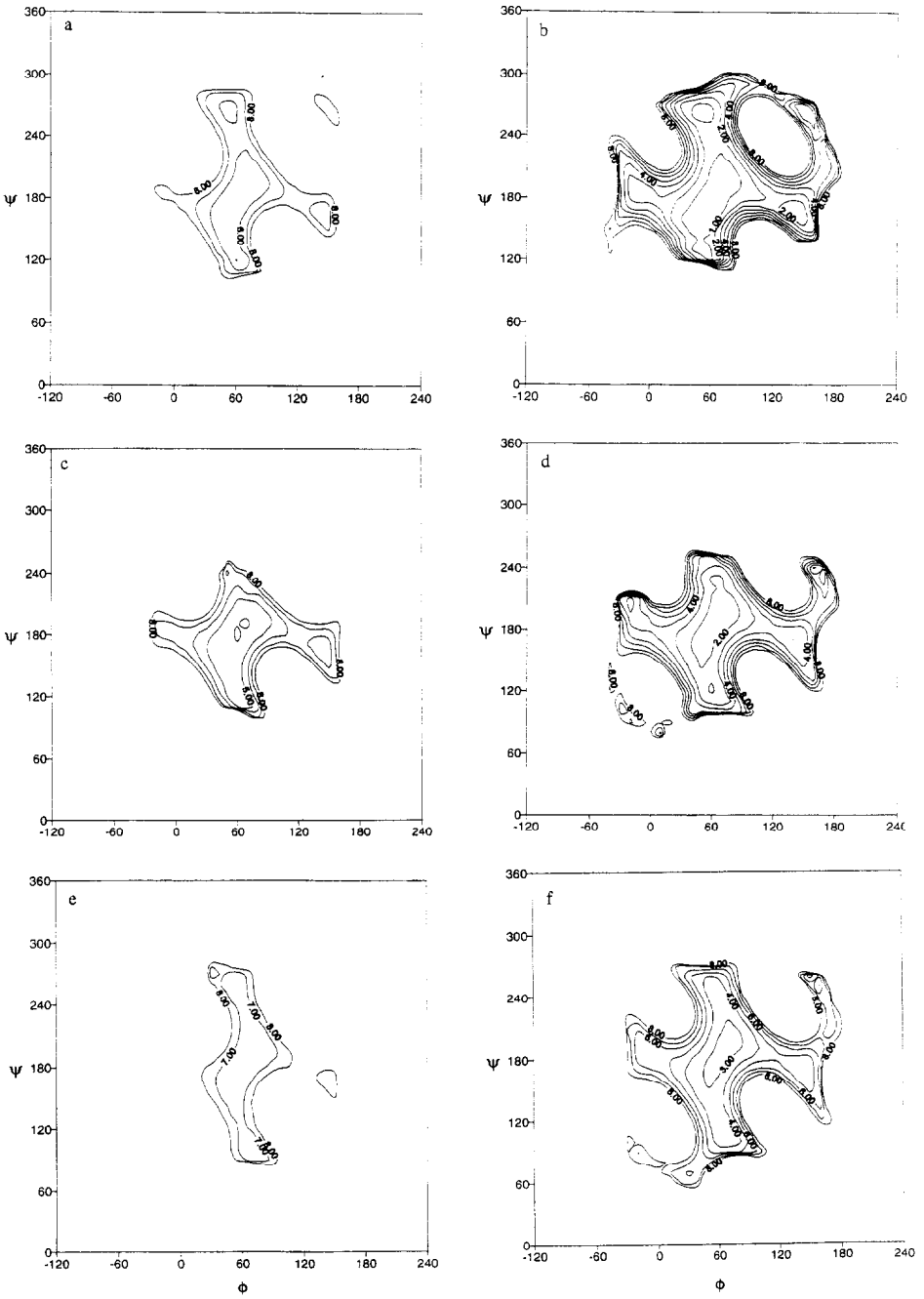

Fig. 1. The (ϕ, ψ) ECEPP maps for β-gentiobiose at constant ω: (a) $\omega = 0°$, (b) $\omega = 60°$, (c) $\omega = 120°$, (d) $\omega = 180°$, (e) $\omega = 240°$, and (f) $\omega = 300°$ (analogous to Fig. 5 of ref. [18]). Energy levels are countered at 1 kcal/mol increments to 8 kcal/mol above the global energy minimum. The energies and the (ϕ, ψ, ω) values in the minima were as follows: (b) −4.18 kcal/mol (69°, −168°, 67°); (d) −3.60 kcal/mol (71°, −163°, 179°); (f) −3.34 kcal/mol (70°, −165°, −63°).

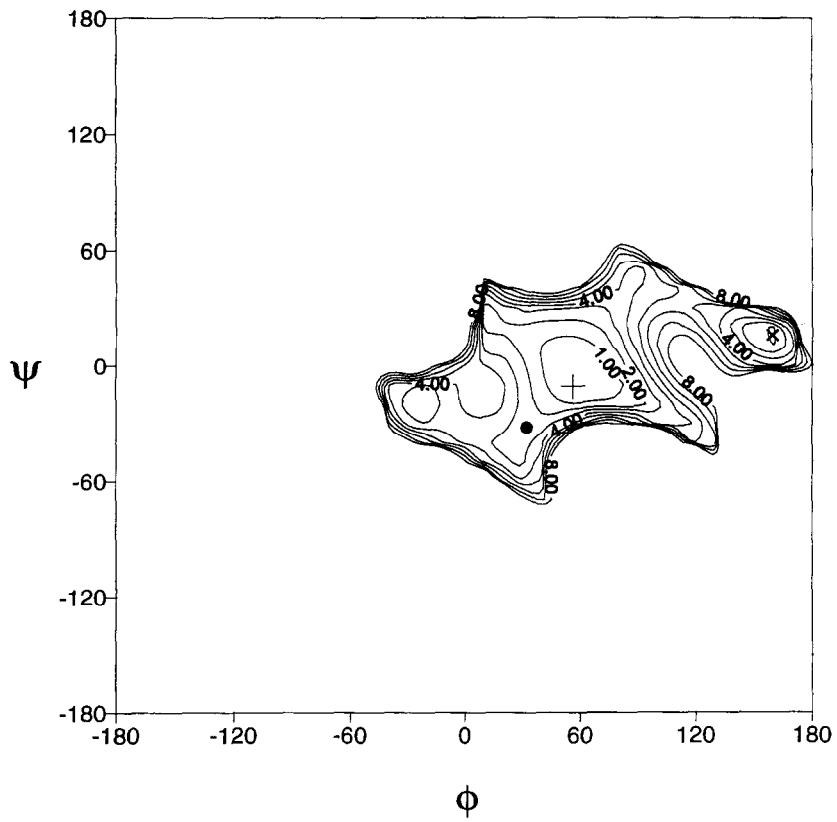

Fig. 2. The (ϕ, ψ) ECEPP map for β-laminarabiose (analogous to Fig. 5 of ref. [20]). Energy levels are countered at 1 kcal/mol increments to 8 kcal/mol above the global energy minimum. The energies and the (ϕ, ψ, ω) values in the minima were as follows: the global minimum −5.12 kcal/mol (58°, −14°); the second lowest −2.65 kcal/mol (158°, 16°). The global energy minimum is marked with (+), the second lowest energy minimum is marked with (×), and the crystal conformation [21] of the molecule is marked with (●).

ods this method uses internal coordinates (bond lengths, bond angles, and dihedral angles) as variables and the Lagrange–Hamilton formalism for describing molecular motion [22].

The distinctive feature of this approach is the possibility to simulate internal motions of polymeric molecules as chains or trees of rigid bodies, that is, with the minimum number of internal degrees of freedom. For oligosaccharides, this means that one does not have to take into account the relative motion of atoms within glucosidic rings. As a result, the time step of molecular dynamics can be increased, thus significantly increasing the efficiency of sampling in conformational space, at least in the case of small chain molecules. Recent studies have shown that, for the small oligopeptide–Met-enkephalin, it was possible to cover a very large portion (if not all) of the conformational space of the molecule, including all conformations observed experimentally [23].

The ICSD runs were for a single oligosaccharide molecule in vacuum. The starting conformations were obtained by conjugate gradient minimization from the unfolded (all torsion at 180°) structures. Heating to 300 K was done by a short ICSD run of 100 steps. After that the temperature was fixed at 300 K as described elsewhere [23]. A time step of 0.015 ps was used for all ICSD experiments. Every 250 steps during the trajectory the conformation was saved and minimized by 50 steps of conjugate gradient minimization in order to select individual conformational states of the molecules.

The establishment of the conformational equilibrium in the ICSD experiments was checked by monitoring relative populations of the ten most populated conformational states, as described elsewhere [23]. It was found that trajectories of 22 ns (1,400,000 time steps) were enough to reach the conformational equilibrium for the analogues of HSE (structures **3a** and **3b**). This means that at the end of the specified period the kinetic curves of relative populations of different substates reached distinct plateaux. For HSE, a trajectory approximately two times longer was calculated (43 ns). One should note that there is no rigorous way to ensure that the populations of conformational substates have reached the global equilibrium during a molecular dynamics simulation. It is only possible to check that the trajectory is not trapped in one of the substates but wanders between them. In this case plateaux on the kinetic curves of relative populations indicate that the local equilibrium between these substates has been reached. We checked also that random selection of the starting point for the trajectory did not change significantly the ordering and the populations of the most frequently visited states in the equilibrium distribution.

Classification of conformational states.—Selection of distinct conformational states is a complex problem even for relatively small polymeric molecules. There is no standard approach to this problem and it is necessary to find some specific features of the molecules studied that can be used for classification of the many hundreds of thousands of conformations from the ICSD trajectory.

Preliminary visual analysis of several low-energy conformations of HSE showed that: (*i*) three central residues of the β-(1 → 6) backbone completely define the shape of the molecule; (*ii*) terminal backbone and side-chain residues are very labile, but their conformations have little, if any, influence on overall molecular shape; (*iii*) most of the low-energy conformations are compact structures with parallel or antiparallel orientation of the second and fourth backbone glucosidic rings.

Based upon the above observations we have selected the following two parameters for classification of the possible conformational states of the molecules studied. (1) The distance between approximated centres of the second and fourth backbone glucose residues (the centres are taken at the mid-point of a virtual bond that connects C-2 and C-5 atoms of the rings; this value is denoted as d). (2) The dihedral angle between the (C2, C3, C5) planes of these two residues, denoted as α.

In the population map of HSE (Fig. 3), each point represents a conformation saved during the ICSD calculations. There are several regions where points form well-defined clusters. At the first stage of the analysis we have selected these clusters as individual conformational states of the molecule. However, more careful analysis showed that in some cases these clusters can involve dissimilar conformations, with more than 60° differences in ϕ, ψ, and ω angles of the molecule backbone. Therefore, in order to

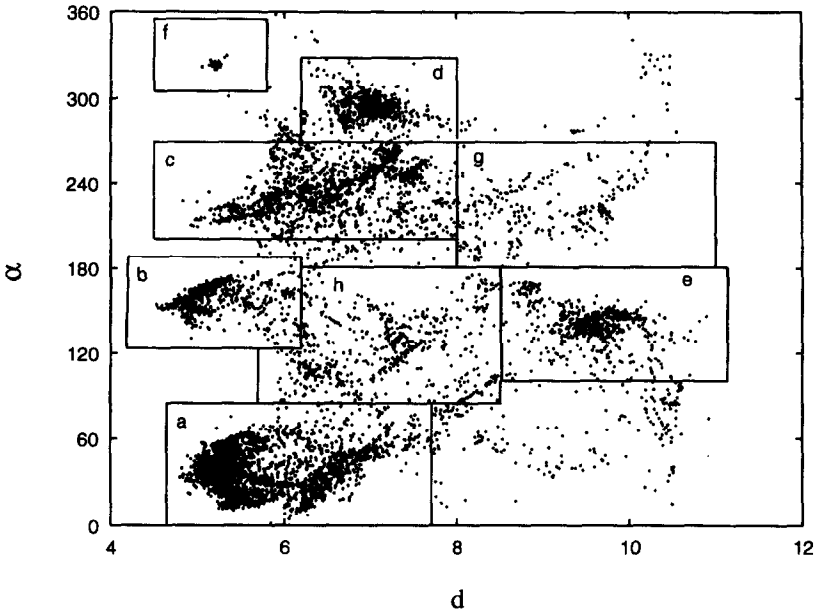

Fig. 3. The α, d (degrees, Å) map of the 42 ns ICSD trajectory of HSE. Each point corresponds to a conformation stored on the trajectory and quenched by a short energy minimization (see Experimental section). Regions selected for the classification of individual states of the molecule are shown by rectangles.

obtain more accurate separation of the different conformational states of the molecule, we decided to use standard (ϕ, ψ) maps.

We have built up (ϕ, ψ), (ψ, ω), and (ϕ, ω) population maps for second and third β-(1 → 6) bonds of the backbone. It was found that angle ψ was useless for our purposes because this angle varied over a wide range (−90° to 90°) and did not give any distinct clusters (data not shown). At the same time (ϕ, ω) maps had several well-defined spots (Fig. 4) for two central β-(1 → 6) glucosidic bonds of HSE. These maps were used for more accurate separation of the conformational states that belong to the same clusters on (d,α) maps.

Thus, conformational states of the molecule are denoted by a code, XYYZZ, where X is the label of the spots on the (d, α) map, YY is the two-figure code of the spot on the (ϕ, ω) map of the second β-(1 → 6) linkage, ZZ is the code of the spot on the (ϕ, ω) map of the third β-(1 → 6) linkage. The established nomenclature using *gauche, trans,* and *cis* descriptors for the position of O-6 in β-(1 → 6)-linked disaccharides can be related to marked sectors on the (ϕ, ω) maps as follows: sectors 11, 21, 31; 12, 22, 32; and 13, 23, 33 correspond to *trans–gauche, gauche–gauche,* and *gauche–trans* orientations, respectively.

3. Results and discussion

Conformational states of HSE.—Table 1 presents the general characteristics of all conformational states observed in the ICSD calculations. The most frequently found

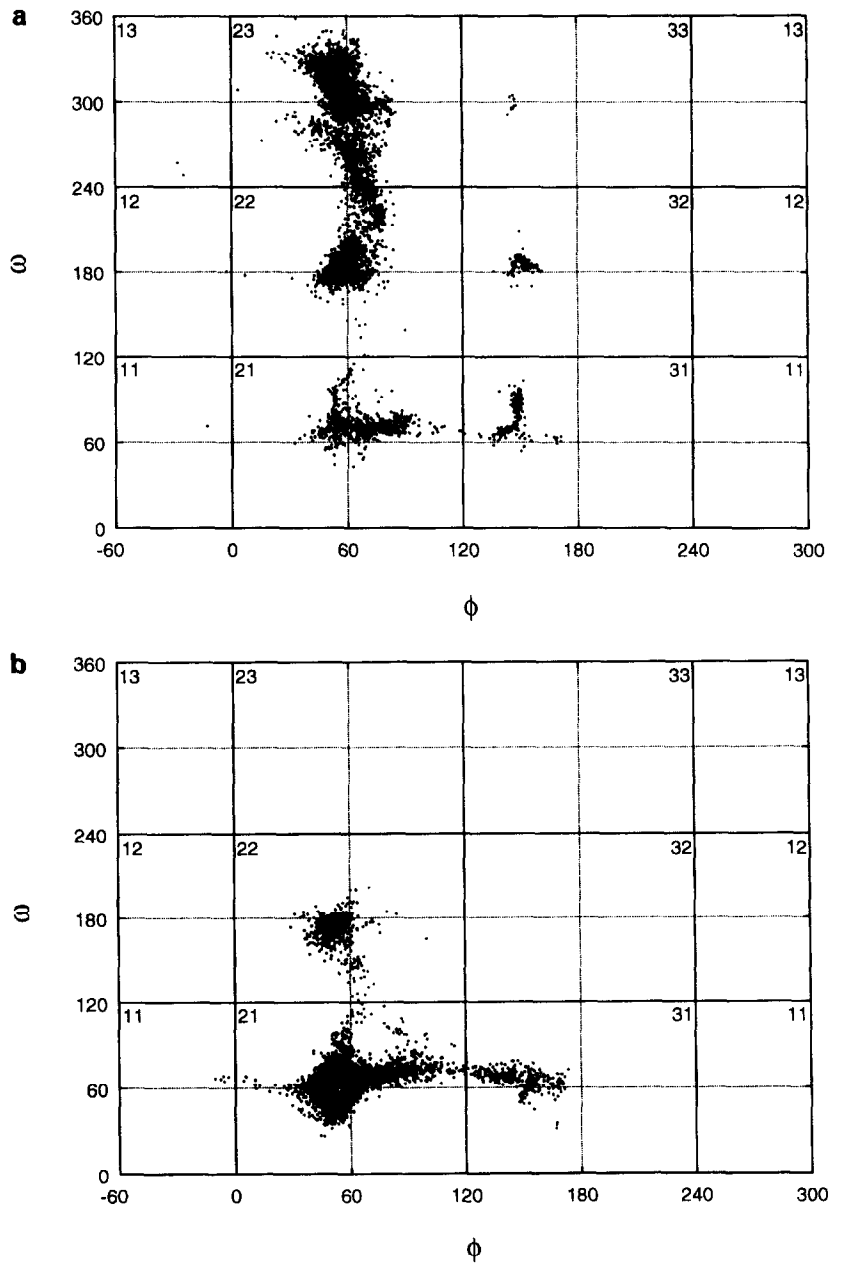

Fig. 4. The (ϕ, ω) maps of the 42 ns ICSD trajectory of HSE. (a) The map for the β-(1 → 6)-glycosidic bond between G_2 and G_3 of the backbone; (b) the map for the β-(1 → 6)-glycosidic bond between G_3 and G_4 of the backbone. Each point corresponds to a conformation stored on the trajectory and quenched by a short energy minimization (see Experimental section). Regions selected for the classification of individual states of the molecule are shown by rectangles.

Table 1
Statistics for selected conformational states of HSE (1)

Code of conf. state	Population	Lowest energy (kcal/mol)	Average energy (kcal/mol)	Average d [a] (Å)	Average α [a] (°)
a2321	4258(42.5%)	−9.479	−6.868	5.71(0.52)	37.31(12.3)
d2322	1006(10.0%)	−9.475	−6.818	7.14(0.27)	293.96(7.5)
c2221	834(8.3%)	−8.755	−6.225	6.53(0.76)	230.18(18.5)
e2121	497(4.9%)	−8.407	−5.833	9.87(0.47)	134.61(13.0)
c2321	472(4.7%)	−7.692	−5.876	6.66(0.54)	234.28(18.5)
b2221	310(3.1%)	−8.509	−6.332	5.23(0.37)	156.55(9.7)
b2321	245(2.4%)	−8.475	−6.325	5.32(0.34)	160.55(9.4)
d2321	136(1.3%)	−8.421	−6.205	6.71(0.32)	301.74(13.3)
c3121	130(1.3%)	−8.596	−6.735	7.56(0.22)	247.49(8.8)
a2231	80(0.8%)	−7.527	−5.919	6.41(0.45)	60.31(11.1)
d2331	66(0.6%)	−8.524	−6.392	7.05(0.28)	290.74(8.7)
g3121	60(0.6%)	−7.838	−6.118	9.30(0.47)	221.04(10.2)
g2121	52(0.5%)	−7.403	−5.461	9.50(0.50)	215.01(14.1)
c3221	48(0.4%)	−6.531	−5.340	7.36(0.30)	235.82(15.8)
c2331	44(0.4%)	−7.764	−5.691	6.61(0.44)	245.00(13.1)
f2321	43(0.4%)	−7.893	−6.477	5.28(0.21)	327.75(9.1)
g2321	42(0.4%)	−6.800	−5.051	8.91(0.26)	207.29(13.9)
d2221	22(0.2%)	−7.469	−6.333	7.58(0.26)	281.47(7.3)
g2221	19(0.1%)	−6.469	−5.205	8.81(0.29)	230.85(10.6)

[a] Estimated standard deviations in parentheses.

structures account for 83% of the trajectory. The remaining 17% is occupied mostly by unfolded conformations that cannot be related to any fairly stable conformational states of the molecule. Visual analysis of the most frequently occurring conformations showed, however, that there are only three structural motifs adopted by the molecule, namely, antiparallel (a2321), crossed (d2322, c2321, b2321, d2321), and parallel (c2221, b2221, c3121). Stereopairs of representative conformations are shown in Fig. 5.

The most populated antiparallel structure (a2321) accounts for almost half of the trajectory and it is characterized by close location of both the terminal backbone residues and the β-(1 → 3) branch residues. Thus G_1 is in close contact with G_7, and G_5 is in close contact with G_6. The torsion angles (°) (ϕ, ψ, ω) of the two central backbone glucosidic bonds are (56, 249, −55) and (49, 148, 54) for the second and the third glucosidic bonds, respectively. Most low-energy conformations that were found in ICSD calculations are related to this structure. The average energy of this state is also the lowest. In addition, this conformational motif is extendable, that is, it can occur in longer polysaccharides containing the same fragment.

Although, as we noted above, the relative contribution of hydrogen bonding to the stability of conformations in our calculations was underestimated, we believe it is useful to list the specific intramolecular hydrogen bonds that are characteristic for particular substates. The antiparallel conformation can be stabilized by a network of hydrogen bonds: O-2/G_1–O-2/G_7; O-2/G_1–O-3/G_7; O-4/G_6–O-3/G_5; O-6/G_6–O-2/G_4; and O-6/G_6–O-4/G_5.

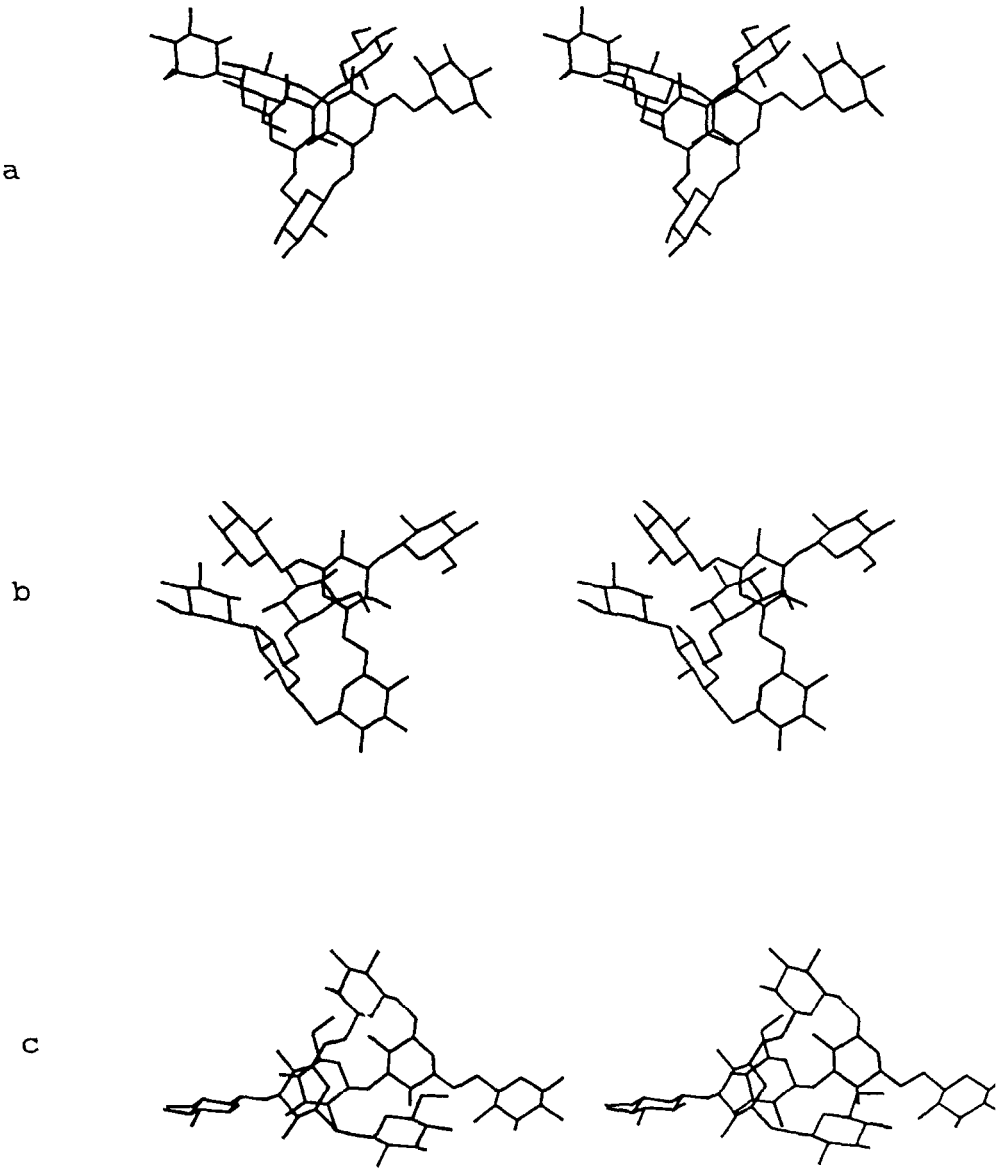

Fig. 5. Stereopairs of representative conformations of HSE corresponding to the most populated conformational motifs. (a) The antiparallel conformation (a2321); (b) the crossed conformation (c2321); (c) the parallel conformation (c2221). For each state the conformation with the lowest energy encountered on the ICSD trajectory is presented.

Crossed structures (d2322, c2321, b2321, d2321) occur second most often, about 18.5% of the time. This set of conformational states is characterized by two features: glucose rings of the second and fourth backbone residues are perpendicular to each other

and the fifth residue is located between G_1 and G_6. There are several possibilities for forming hydrogen bonds between hydroxyl groups of G_5 and closely located G_1 and G_6, namely, O-1/G_5–O-4/G_6, O-1/G_5–O-2/G_1, O-2/G_5–O-2/G_1 (d2322 state); O-3/G_5–O-2/G_1, O-4/G_5–O-2/G_6 (b2321 state), and O-1/G_5–O-3/G_6, O-3/G_5–O-3/G_1 (d2321 state). The number of possible hydrogen bonds is half as large as for the antiparallel structure. The β-(1 → 3) branch residue at the fourth position is not involved in intramolecular interactions. We suppose that crossed conformational states can be considered intermediate structures of low stability between antiparallel and parallel ones.

Parallel structures (c2221, b2221, c3121) occupy the third most frequently visited conformational motif. They account for 12.7% of the trajectory and are characterized by parallel orientation of the glucose rings of the second and fourth backbone residues, and close positions for G_1 and G_5, and G_6 and G_7. The possibilities of forming hydrogen bonds are fewer than antiparallel structure. One hydrogen bond can be formed for each pair of close residues (O-3/G_1–O-4/G_5 and O-2/G_6–O-3/G_5) with no possibility of a hydrogen bond network.

Conformational states of the hexasaccharide analogue **3a** *of HSE.*—All conformational states selected from the ICSD experiment are presented in Table 2. Compact structures are also most populated but there are only two main types of compact structures in this case. In the nomenclature of conformational states of HSE, these are antiparallel (a2321, h2321) and parallel (c2221, b2221) ones. These structures are characterized by close contacts between G_6 and G_1 and G_6 and G_5, respectively. The other conformational states, e2121, f2121, e2321, f2131, are unfolded rather than compact, but they are stable and well populated. These eight states account for 65% of the trajectory. Stereopairs of the lowest energy conformations for antiparallel and parallel conformations of this molecule are presented in Fig. 6. No crossed conforma-

Table 2
Statistics for selected conformational states of the hexasaccharide analogue **3a** of HSE

Code of conf. state	Population	Lowest energy (kcal/mol)	Average energy (kcal/mol)	Average d [a] (Å)	Average α [a] (°)
a2321	1123(21.2%)	−7.708	−5.720	5.50(0.31)	47.27(11.51)
e2121	594(11.2%)	−7.020	−5.018	10.06(0.72)	134.33(14.23)
h2321	494(9.3%)	−6.743	−4.863	7.14(0.63)	54.51(18.74)
f2121	436(8.2%)	−6.461	−4.882	10.49(0.34)	68.93(26.45)
c2221	379(7.1%)	−8.153	−5.651	5.65(0.49)	221.44(11.33)
b2221	283(5.3%)	−7.797	−5.854	5.32(0.40)	151.03(13.64)
e2321	75(1.4%)	−5.706	−4.483	8.98(0.41)	132.26(15.87)
f2131	39(0.7%)	−5.754	−4.585	10.43(0.24)	62.91(18.76)
f2122	32(0.6%)	−5.548	−4.124	10.73(0.37)	55.55(19.81)
b2321	21(0.4%)	−5.458	−4.717	5.48(0.44)	149.34(18.65)
h2322	18(0.3%)	−5.556	−4.824	6.82(0.31)	83.19(10.32)
h2122	15(0.2%)	−5.302	−3.912	7.77(0.37)	64.69(12.37)
h2231	15(0.2%)	−5.964	−4.762	6.72(0.33)	96.79(10.97)
e2221	12(0.2%)	−6.053	−4.746	8.58(0.31)	139.50(14.36)

[a] Estimated standard deviations in parentheses.

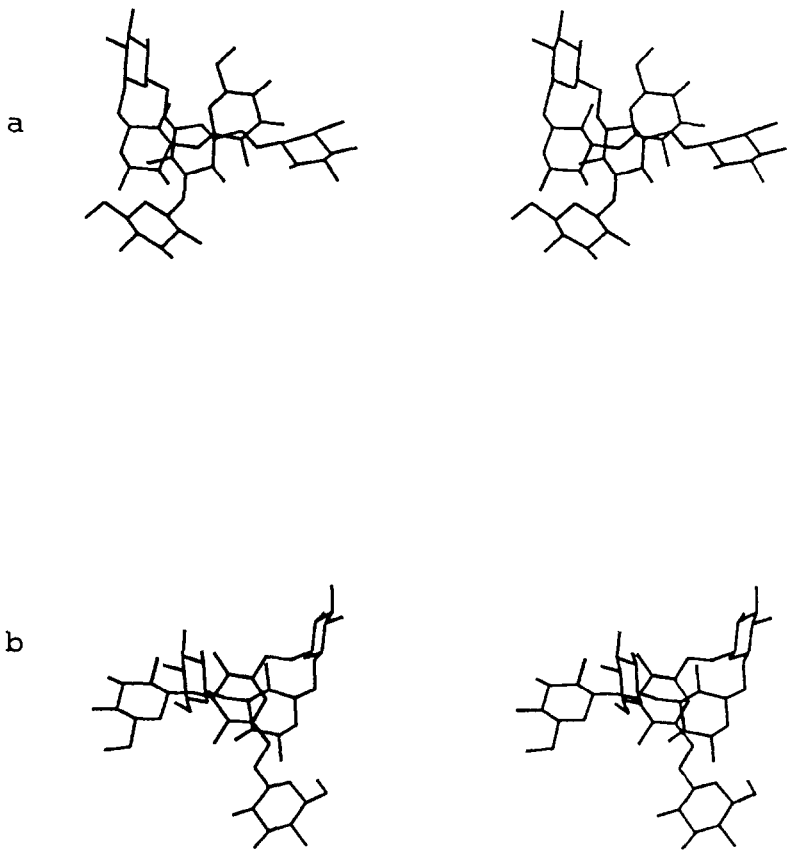

Fig. 6. Stereopairs of representative conformations of the hexasaccharide analogue of the HSE (structure **3a**) corresponding to the most populated conformational motifs. (a) The antiparallel conformation (a2321); (b) the parallel conformation (c2221). For each state the conformation with the lowest energy encountered on the ICSD trajectory is presented.

tions were observed in this case, probably because of the lack of a fifth backbone residue.

Like HSE, antiparallel structures (a2321, h2321) of the hexasaccharide analogue are also most populated. However, in this case, they account for only 31% of the trajectory. This conformation can also be stabilized by a pair of possible hydrogen bonds: O-2/G_6–O-2/G_1; O-3/G_6–O-2/G_1. The hydroxyl group at C-2 of the first backbone residue can also be involved in hydrogen bonding as both donor and acceptor.

The antiparallel structure has comparatively low energy, but the lowest single state energy and the lowest average energy are observed for the parallel conformation. A possible reason for this is the additional hydrogen bond that can form between the free hydroxyl group at C-1 of G_4 and the CH_2OH group of the first backbone residue. Such a hydrogen bond could form in the antiparallel case between the CH_2OH group of G_5 and the free hydroxyl at C-1 of G_4, but it is not sterically possible because of

Table 3
Statistics for selected conformational states of the heptasaccharide analogue **3b** of the HSE

Code of conf. state	Population	Lowest energy (kcal/mol)	Average energy (kcal/mol)	Average d [a] (Å)	Average α [a] (°)
b2231	1200(22.7%)	−9.202	−7.161	6.48(0.32)	113.97(11.52)
d2321	1014(19.2%)	−9.111	−6.803	6.32(0.27)	251.78(23.04)
c2321	442(8.3%)	−9.708	−6.984	5.44(0.34)	163.32(11.18)
c2221	361(6.8%)	−9.493	−7.250	5.46(0.43)	159.45(9.12)
a2321	228(4.3%)	−8.616	−6.562	6.16(0.69)	35.17(15.31)
b2221	205(3.8%)	−8.953	−6.858	6.29(0.47)	125.37(10.97)
e2221	202(3.8%)	−8.222	−6.239	7.74(0.35)	229.88(18.02)
e2321	192(3.6%)	−7.995	−5.763	7.50(0.37)	235.27(21.71)
g2321	162(3.0%)	−7.871	−6.160	8.05(0.31)	87.66(18.35)
f2221	150(2.8%)	−8.547	−5.787	8.81(0.46)	248.54(16.60)
d2221	123(2.3%)	−8.507	−6.318	6.31(0.31)	219.21(19.98)
h2321	119(2.2%)	−7.964	−5.869	9.08(0.31)	127.94(19.67)
b2222	100(1.9%)	−8.734	−6.483	6.92(0.30)	100.16(11.32)
f2321	74(1.4%)	−7.168	−5.381	8.81(0.39)	225.22(14.16)
a2231	66(1.2%)	−8.679	−6.659	6.09(0.50)	58.22(10.54)
b2321	46(0.8%)	−7.582	−6.005	6.28(0.57)	122.65(15.36)
a2223	29(0.5%)	−6.791	−5.221	5.70(0.60)	30.47(11.33)
b3221	24(0.4%)	−8.499	−6.829	6.90(0.31)	115.51(16.25)
d3221	22(0.4%)	−7.345	−6.112	6.33(0.44)	254.64(17.48)
g2222	17(0.3%)	−7.104	−5.883	7.84(0.22)	103.01(14.40)
g2231	15(0.2%)	−6.870	−5.783	7.75(0.24)	101.63(17.16)
e3221	15(0.2%)	−8.418	−6.368	7.30(0.38)	221.83(10.73)

[a] Estimated standard deviations in parentheses.

insufficient length of the β-(1 → 3) bond. The O-2/G_6–O-2/G_5 hydrogen bond may also stabilize the parallel structure.

Conformational states of the heptasaccharide analogue **3b** *of HSE.*—Compact structures are also most populated here, but the conformational properties of the molecule drastically differ from the two cases above. In terms of conformational states of HSE, the crossed structures (b2231, d2321, c2321, c2221, b2221, d2221, b2222, b2321, and e2321) are most populated and account for approximately 70% of the ICSD trajectory. These structures are characterized by close location of the fifth backbone residue to both G_1 and G_5. There are several possibilities to form hydrogen bonds in these structures, namely, O-1/G_5–O-2/G_1 and O-2/G_5–O-2/G_6 (b2231); O-1/G_5–O-2/G_6 (d2321); O-1/G_5–O-3/G_1 and O-3/G_5–O-2/G_6 (c2321 and c2221).

Fig. 7. Stereopairs of representative conformations of the heptasaccharide analogue of the HSE (structure **3b**) corresponding to the most populated conformational motifs. (a) The crossed conformation (b2231); (b) the antiparallel conformation (a2321); (c) the unfolded 5-1 conformation (e2221); (d) the unfolded 5-6 conformation (g2321). For each state the conformation with the lowest energy encountered on the ICSD trajectory is presented.

a

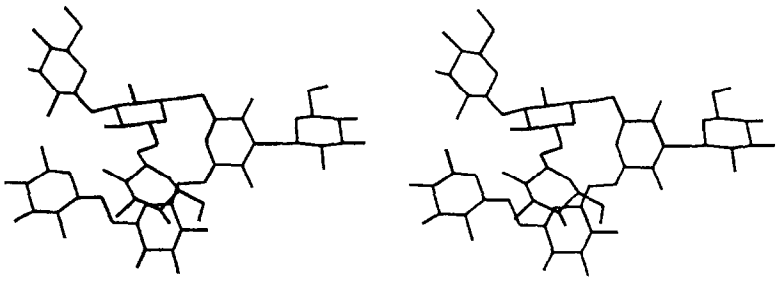

b

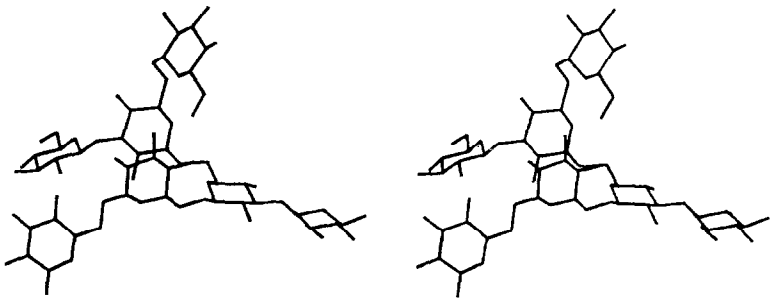

c

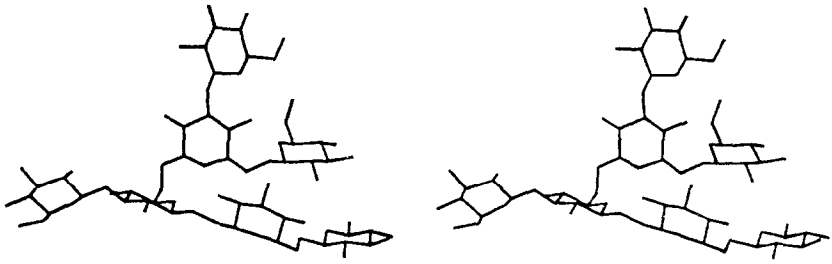

d

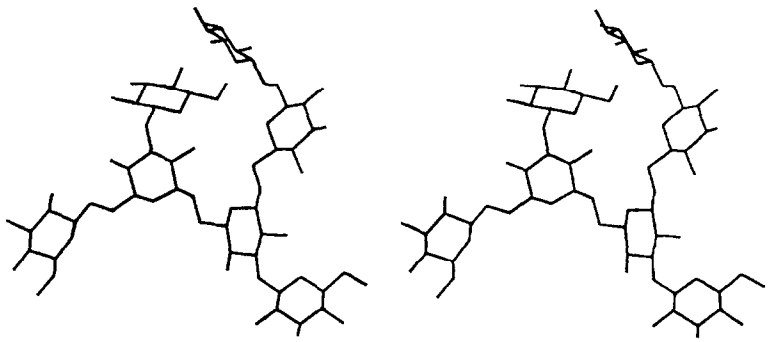

The rest of the trajectory can be related to three different sets of conformational states: antiparallel (a2321, a2231, and a2223), unfolded 5-1 (e2221 and f2221), and unfolded 5-6 (g2321, h2321, and f2321). Each of these occupies approximately 6% of the trajectory. Their populations are equal within the accuracy of our calculations.

All conformational states selected from ICSD are presented in Table 3. Stereopairs of representative conformations of the above-mentioned conformational motifs are presented in Fig. 7. These states account for 89% of the trajectory.

Antiparallel structures have exactly the same properties and hydrogen bonding possibilities as those of the a2321 state of the hexasaccharide analogue of HSE. 5-1 and 5-6 are two sets of rather unfolded conformations that have common conformational motifs (close contacts between G_5 and G_1, and between G_5 and G_6, respectively). These states have relatively high energy and only a small possibility of forming hydrogen bonds.

Comparison with literature experimental data.—We are unaware of any experimental data on the spatial structure of β-(1 → 3) branched β-(1 → 6) gluco oligomers. Comparison of results of the molecular dynamics with low energy minima calculated for β-gentiobiose using the MM3 potential [18] shows that the most frequently visited conformational states found in this work for HSE and its analogues commonly are combinations of the three lowest energy regions predicted by MM3 calculations. The crystal structure of β-gentiobiose resides in the highly populated zone 22.

There are a few exceptions, however, that clearly demonstrate predominant influence of non-local tertiary interactions upon the observed populations. One may see in Fig. 4a, for instance, that an eclipsed conformation with $\omega = 240°$ between states 22 (*gg*) and 23 (*gt*) is considerably populated, although both on ECEPP (Fig. 1) and MM3 [18] energy maps for gentiobiose this region has the highest energy among eclipsed conformations (several kcal/mol above all local minima). In Fig. 4b, one may see that the *gt* minimum corresponding to region 23 is not populated at all while it is the most populated one in Fig. 4a.

As we noted in the Introduction, various analogues of HSE were extensively tested for biological activity, including oligosaccharides **3a** and **3b** chosen for the present study. Hexasaccharide **3a** has approximately the same activity as HSE. In contrast, heptasaccharide **3b** with a shifted β-(1 → 3) branch has approximately 1000 times lower activity than HSE [6]. These experimental facts can be correlated with the results of our ICSD simulation, if one assumes that the antiparallel structure described above is responsible for elicitor activity. This conclusion is supported by the following considerations. The antiparallel motif is the most populated conformational state for both active

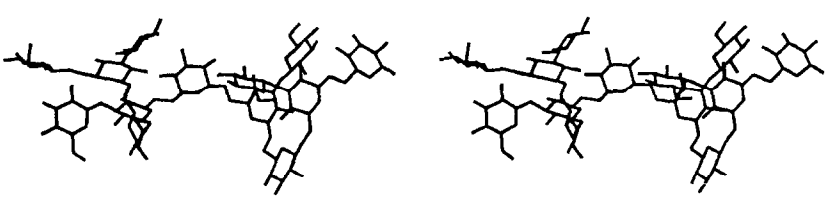

Fig. 8. Concatenation of two antiparallel structures of HSE in a longer polysaccharide chain.

molecules, and this conformational state is weakly populated in the case of the inactive analogue. Secondly, it is known that increasing the β-(1 → 3) branch length, at least at the reducing terminus, has no influence on elicitor activity of the molecule [6]. One can see from Fig. 5a that antiparallel conformations impose no restrictions on the chain lengths of the β-(1 → 3) branches. Thirdly, this conformation must be sensitive to substitution of G_1 and G_6 for *N*-acetyl-glucosamine, which is known to inactive the molecule. Such substitutions are likely to disturb the characteristic hydrogen bond network of this structure. And finally, the conformation is extendable from both backbone ends and can be repeated in similar longer chains (see Fig. 8 for instance).

Based upon the above arguments we conclude that the antiparallel structure presented in Fig. 5a is a likely candidate for the elicitor-active conformation.

References

[1] N.T. Keen, *Science*, 187 (1975) 7–12.
[2] K. Cline and P. Albersheim, *Plant. Physiol.*, 68 (1981) 221–228.
[3] P. Albersheim and A.G. Darvill, *Sci. Am.*, 253 (1985) 58–64.
[4] A.R. Ayers, J. Ebel, B. Valent and P. Albersheim, *Plant. Physiol.*, 57 (1976) 751–774.
[5] J.K. Sharp, M. McNeil, and P. Albersheim, *J. Biol. Chem.*, 259 (1984) 11321–11336.
[6] M.G. Hahn, J.J. Cheong, W. Birberg, P. Fugedi, A. Piloti, P. Garegg, N. Hong, Y. Nakahara, and T. Ogawa, *NATO ASI Series*, H36 (1989) 91–97.
[7] P. Ossowski, A. Pilotti, P. Garegg and B. Lindberg, *J. Biol. Chem.*, 259 (1984) 11337–11340.
[8] J.K. Sharp, P. Albersheim, P. Ossowski, A. Pilotti, P. Garegg, and B. Lindberg, *J. Biol. Chem.*, 259 (1984) 11341–11345.
[9] H. Takeda, N. Yasuoka, and N. Kasai, *Carbohydr. Res.*, 53 (1977) 137–152.
[10] F.A. Momany, R.F. MacGuire, A.W. Burgess, and H.A. Scheraga, *J. Phys. Chem.*, 79 (1975) 2361–2381.
[11] G. Nemethy, M.S. Pottle, and H.A. Scheraga, *J. Phys. Chem.*, 87 (1983) 1883–1887.
[12] M.J. Sippl, G. Nemethy, and H.A. Scheraga, *J. Phys. Chem.*, 88 (1983) 6231–6233.
[13] M.G. Petukhov and V.L. Pershin, *Zh. Struct. Khim. (USSR)*, 29 (1988) 167–168.
[14] M.R. Pincus, A.W. Burgess and H.A. Scheraga, *Biopolymers*, 15 (1976) 2485–2521.
[15] I. Simon, H.A. Scheraga, and R. St. J. Manley, *Macromolecules*, 21 (1988) 983–990.
[16] A. Duben, M. Hricovini, and I. Tvaroska, *Carbohydr. Res.*, 247 (1993) 71–81.
[17] G.M. Lipkind, V.E. Verovsky and N.K. Kochetkov, *Carbohydr. Res.*, 133 (1984) 1–13.
[18] M.K. Dowd, P.J. Reilly, and A.D. French, *Biopolymers*, 34 (1994) 625–638.
[19] D.C. Rohrer, A. Sarco, T.L. Bluhm, and Y.N. Lee, *Acta Crystallogr., Sect. B*, 36 (1980) 650–654.
[20] M.K. Dowd, A.D. French, and P.J. Reilly, *Carbohydr. Res.*, 233 (1992) 15–34.
[21] C. Woodcock and A. Sarko, *Macromolecules*, 13 (1980) 1183–1187.
[22] A.K. Mazur and R.A. Abagyan, *J. Biomol. Struct. Dyn.*, 6 (1989) 815–832.
[23] V.E. Dorofeyev and A.K. Mazur, *J. Biomol. Struct. Dyn.*, 10 (1993) 143–167.